FAILURE OF ADHESIVELY BONDED JOINTS. ANALYSIS OF EXPERIMENTAL RESULTS BY NOMINAL AND LOCAL APPROACHES.

A. Barroso, F.París, V. Mantič

Group of Elasticity and Strength of Materials, School of Engineering, University of Seville,
Camino de los Descubrimientos s/n, Sevilla, Spain.

ABSTRACT

The failure in structural adhesively bonded lap joints can be analyzed following different approaches: using a nominal stress state typically given by Strength of Material models, a local singular stress state induced at the multimaterial corners of the joint, or using cohesive constitutive laws for the adhesive layer or other damage progression models. The aim of this paper is to analyze the suitability of models based on local stress states to predict a failure in metal-to-composite double-lap joints and their capability to predict a failure when the geometrical parameters such as overlap length, adherent thickness or stacking sequence change. For this objective, a preliminary test program has been carried out, which has shown some limitations in approaches using local stress states when a gross yielding takes place.

1.- INTRODUCTION

The failure prediction of adhesively bonded lap-joints between composite materials is a complex problem, Mathews *et al* [1]. There exist different approaches, some of them based on either the nominal stress state, typically evaluated by means of the Strength of Materials formulas, or the local (singular) stress state at the multimaterial corners which appear in the overlap zone. There are also other approaches, such as Continuum Damage Mechanics, which try to characterize the failure process using more complex constitutive laws.

Among the approaches based on nominal stress states the work by Hart-Smith [2] is an excellent example. Hart-Smith found, for example, that in double lap joints in tension the failure key parameter is the strain energy in shear per unit lap-area. This fact was successfully confirmed by the experimental results by Leman and Hawley [3]. Crocombe [4] proposed an alternative criterion based on a plastic collapse mechanism in the adhesive layer. Kairouz [5] studied the role of the stacking sequence in the failure of composite lap joints. Adams and co-workers have investigated in depth the role of the adhesive fillet in the failure, Adams *et al* [6], and have improved analytical models for the stress analysis of the adhesive joints, Adams and Mallick [7].

The approaches based on the local (singular) stress states have also been widely investigated in literature. The presence of points, in the overlap zone of the joint, where both geometry and mechanical properties change abruptly have attracted attention of several studies to the analysis of the singular stress state induced at these corners and their influence on the initiation of failure. Some of these proposals were based on the presence of a crack at the corner, Ferlund and Spelt [8], or use interfacial fracture mechanics concepts, Hutchinson and Suo [9]. Singular stress states at these points, not considering previous cracks emanating from the corner tip, were analyzed by Gradin [10], Groth [11], Hattori [12], Reedy [13], Reedy and Guess [14], Lefebvre *et al* [15] and Quaresimin and Ricotta [16]. Other works not directly related with adhesive joints but with general corner problems are useful in our problem as they provide powerful techniques and methods for asymptotic stress characterization, e.g., Leguillon and

Yosibash [17] or Grenestedt and Hallstrom [18] analyzing the presence of a very small crack at the notch tip and found a relationship between the stress intensity factor of this small crack and the stress intensity factor of the uncracked corner.
Other approaches, e.g., use a progressive anisotropic degradation of the material, Laschet and Stas [19], define a critical damage zone length by using Finite Elements, Sheppard *et al.* [20], or use cohesive models, Mohammed and Liechti [21].
The objective of the present work is to check the representativity of the singular stress field in the failure of composite to metal double lap joints. In Section 2, the asymptotic stress field at the different multimaterial corners is evaluated by using a semi-analytical tool developed by the present authors together with numerical Boundary Element Method (BEM) models. In Section 3, the numerically analyzed geometries are tested in shear by tension using double lap joint specimens, and then, in Section 4, the comparison of numerical and experimental results is discussed.

2.- CHARACTERIZATION OF THE LOCAL (SINGULAR) STRESS FIELD

Let us consider a polar coordinate system (r,θ) centred at the corner tip. Let us assume stress singularities of the type $O(r^{\lambda-1})$, then the asymptotic stress and displacement fields at the corner can be written as a series expansion

$$\sigma_{ij}(r,\theta)=\sum_{k=1}^{n}\frac{K_k}{r^{1-\lambda_k}}f_{ijk}(\theta),\quad u_i(r,\theta)=\sum_{k=1}^{n}K_k r^{\lambda_k}g_{ik}(\theta),\qquad i,j=1,2,3 \tag{1}$$

where λ_k are the characteristic exponents, $(1-\lambda_k)$ being the order of stress singularities, and K_k are the Generalized Stress Intensity Factors (GSIF). Functions $f_{ijk}(\theta)$ and $g_{ik}(\theta)$ are characteristic angular shape functions of the circumferential coordinate θ. It is well known that λ_k, $f_{ijk}(\theta)$ and $g_{ik}(\theta)$ only depend on the local geometry, material properties and local boundary conditions at the corner neighbourhood and can be evaluated analytically, except of the numerical evaluation of roots of an analytic function, in most of the cases, Costabel *et al* [22], Barroso *et al* [23]. Situations which lead to stress singularities different than $O(r^{\lambda-1})$ represent exceptions, see Sinclair [24] for a few examples of singularities of the type $O(r^{\lambda-1}\ln r)$, and will be not considered here for the sake of simplicity.
The computation of GSIF K_k, requires the knowledge of the whole geometry and loading conditions, so for non trivial geometries, numerical models are needed to calculate K_k. The multimaterial corners appearing in a typical metal-to-composite [0/90/0] double lap joint are depicted in Figure 1. The mechanical properties (orthotropic) of the unidirectional composite (AS4/8552) are (E_{11}=141.3 GPa, $E_{22}=E_{33}$=9.58 GPa, $G_{12}=G_{13}$=5.0 GPa, G_{23}=3.5 GPa, $\nu_{12}=\nu_{13}$=0.3, ν_{23}=0.32, $\alpha_1=-1\cdot10^{-6}$ ºC^{-1}, $\alpha_2=\alpha_3=26\cdot10^{-6}$ ºC^{-1}) while the adhesive has (E=3.0 GPa, ν=0.35, $\alpha_1=45\cdot10^{-6}$ ºC^{-1}) and the aluminium (E=68.67 GPa, ν=0.33, $\alpha_1=24.5\cdot10^{-6}$ ºC^{-1}). The evaluation of the characteristic exponents and the angular shape functions was performed by means of a semi-analytical tool developed by Barroso *et al* [23], which is able to deal with multimaterial corners including any number of linearly elastic anisotropic materials, mathematically non-degenerate and degenerate in the framework of Stroh Formalism. The in-plane orders of stress singularities for the corners in Figure 1, computed by this tool, are shown in Table 1. All the characteristic exponents λ_k leading to singular stress

terms in (1) and the first regular (non-singular) term for each corner configuration have been obtained, which is enough for an accurate description of the stress and displacement fields at the corner tip, Barroso [25].

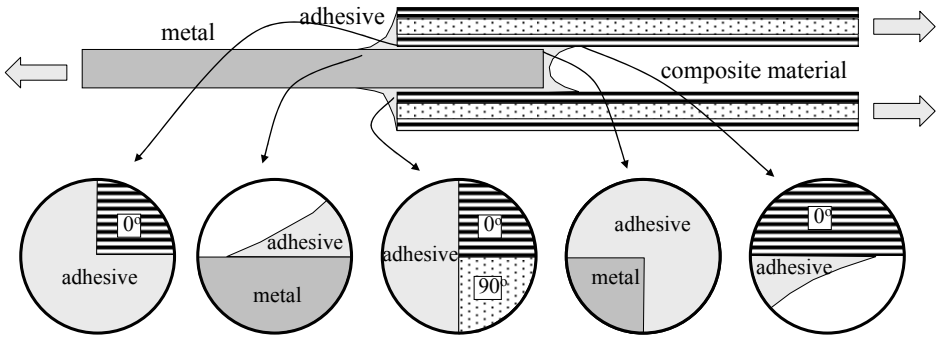

Figure 1.- Multimaterial corners in a composite to metal double lap joint.

It should be stressed that due to the weak singularities (Re(λ)>0.5) obtained for the corners in Figure 1, which are summarized in Table 1, the most singular term alone is not enough for an accurate representation of the stress field, except at an unrealistic close distance to the corner tip, and all terms obtained in Table 1 have to be taken into account.

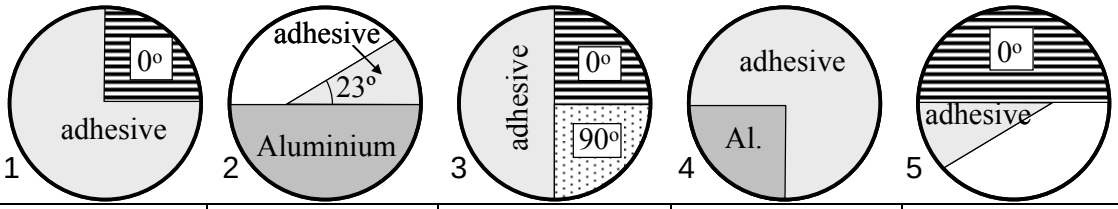

λ_1=0.763236 λ_2=0.889389 λ_3=1.106980	λ_1=0.986914 λ_2=1.926197	λ_1=0.901497 λ_2=1.01447	λ_1=0.686272 λ_2=0.696605 λ_3=0.791014 λ_4=1.152813	λ_1=0.905312 λ_2=1.700273

Table 1.- Characteristic exponents of the multimaterial corners.

In Figure 2 the angular shape functions f_{ijk} and g_{ik} ($i,j=r,\theta$) for corner 1 (see Table 1) and for the first term (λ_1=0.763236) are depicted, the first quadrant of each figure representing the 0º layer of the composite and the rest representing the adhesive, the circumference is the zero reference value for each function. For the sake of brevity not all terms of all corners are shown, but there is huge information obtained from the stress and displacement field divided into the terms of the series expansion in (1).

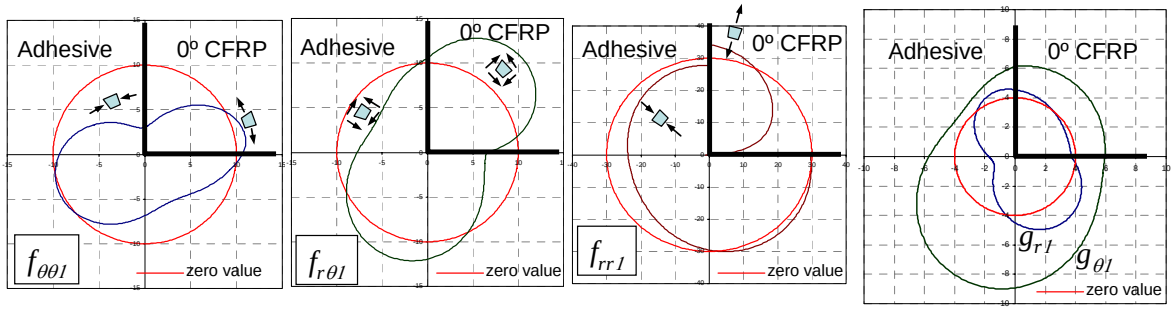

Figure 2.- Angular shape functions f_{ijk} and g_{ik} ($i,j=r,\theta$) for the first term (λ_1) in corner 1.

The contribution of the different terms can be analyzed and the possibility of a failure criteria proposal based on allowable values of the K_k is then opened. The GSIF were obtained for different configurations, shown schematically in Table 2. Both the thickness of the aluminium (1.6 and 3.2 mm) plate and the composite laminate (1.6, 2.2 and 2.9 mm) were changed, also two different stacking sequences were used $[0]_n$ and $[0_n/90_n]_s$. Moreover one configuration had a different overlap length (20 mm instead of 12.5 mm). An aluminium-aluminium configuration was also analyzed.
All these configurations share the same multimaterial corner configurations shown in Table 1, the differences in the global configuration (thickness, stacking sequence, overlap length...) makes the K_k to change while λ_k, $f_{ijk}(\theta)$ and $g_{ik}(\theta)$ do not change as locally the corners do not change, except for the Al-Al case.

	$[0]_8$ (1.6 mm)	$[0]_{12}$ (2.2 mm)	$[0]_{16}$ (2.9 mm)
Al (1.6 mm) L=12.5 mm			
Al (3.2 mm) L=12.5 mm			
Al (3.2 mm) L=20 mm			

	$[0_2,90_2]_s$ (1.47 mm)	$[0_3,90_3]_s$ (2.2 mm)	Al (1.6 mm)
Al (1.6 mm) L=12.5 mm		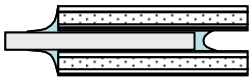	
Al (3.2 mm) L=12.5 mm		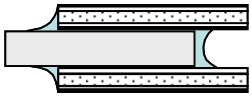	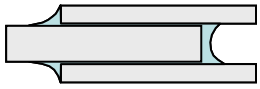

Table 2.- Different configurations numerically simulated using BEM.

Each configuration was numerically analyzed using a BEM code. As an example, a detail of the left hand side of the overlap zone of the BEM model for configuration Al(1.6 mm)/$[0_3/90_3]_s$(2.2 mm), $L_{overlap}$=12.5 mm, is shown in Figure 3.

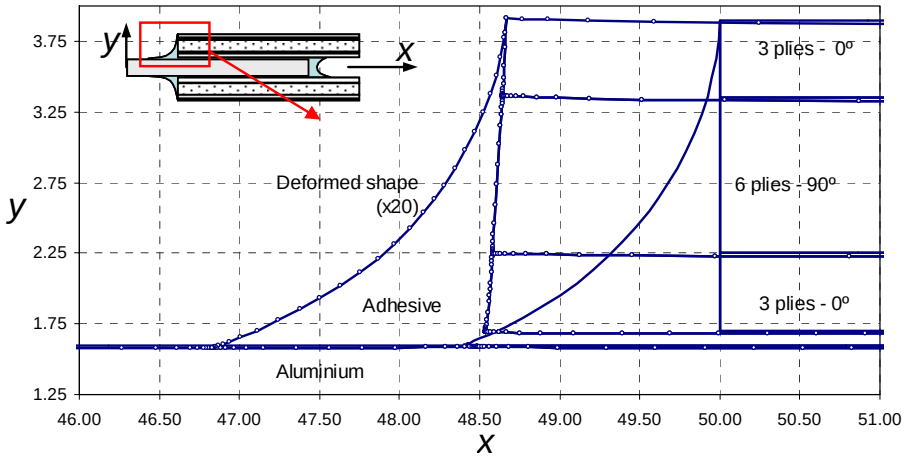

Figure 3.- Detail of the BEM model, deformed and undeformed shape.

The basic features of the BEM model carried out are: linear elastic 2D plane strain, perfect adhesion between the composite layers, the adhesive and the aluminium, a progressive refinement of the mesh towards the corner tip using 10^{-6} and 10^{-8} mm at different corners, uniform temperature effects included (due to the cure cycle of the adhesive) and around 1500 linear elements used. Using a robust least squares procedure, Barroso *et al* [26], the values of the K_k for each corner and for each configuration in Table 1 were numerically computed and normalized following Pageau *et al* [27]. In this procedure, the knowledge of λ_k, $f_{ijk}(\theta)$ and $g_{ik}(\theta)$, with a high accuracy, makes the K_k the only unknowns in (1). The summary of K_k values for the corners 1, 2 and 3, see Table 1, is shown in Table 3, the units being MPa·mm$^{(1-\lambda)}$. Also corner 1 for the Al-Al configuration (#10) is included. Results for corner 3 is obviously only available when the $[0_n/90_n]_s$ stacking sequence is used.

				corner 1 (*corner 1b*)			corner 2		corner 3	
config.	Al	Stack.	Loverlap	k1	k2	k3	k1	k2	k1	k2
1	3.2	$[0^o]_8$	12.5	-0.00275036	0.0273839	-0.0114328	0.000723935	0.000313232		
2		$[0^o]_{12}$	12.5	-0.00265869	0.0296293	-0.0113959	0.000728197	0.000796011		
3		$[0^o]_{16}$	12.5	-0.00267612	0.0319616	-0.0106351	0.000727391	0.00033738		
4	1.6	$[0^o]_8$	12.5	-0.00427067	0.0387508	-0.0171819	0.00134598	0.00118731		
5		$[0^o]_{12}$	12.5	-0.00396993	0.0391659	-0.0165938	0.00138476	0.00121834		
6	3.2	$[0_2/90_2]_s$	12.5	-0.00253126	0.0225756	-0.0100326	0.00088457	0.00017434	0.00357711	0.00188352
7		$[0_3/90_3]_s$	12.5	-0.00258788	0.0263395	-0.0101892	0.000856521	0.000231622	0.00284841	0.00385512
8	1.6	$[0_2/90_2]_s$	12.5	-0.00413257	0.0331505	-0.0158801	0.00168495	0.000276338	0.00481455	0.00140211
9		$[0_3/90_3]_s$	12.5	-0.00418547	0.0347244	-0.0142997	0.00169283	0.000276204	0.00356942	0.00476516
10	3.2	Al 1.6	12.5	*0.00151012*	*-0.0137057*	*0.0310423*	0.00112665	-0.000596641		
11	3.2	$[0^o]_{12}$	20.0	-0.00264264	0.028152	-0.0110226	0.000860062	0.000250501		

Table 3.- GSIF values for the different corners and configurations.

3.- EXPERIMENTAL TESTING

Double-lap shear test were carried out following the requirements of ASTM D3528 [28] for all configurations introduced in Table 2. Two surface treatments were employed for the aluminium plates, namely: anodized and scaled (A and D in Table 4).

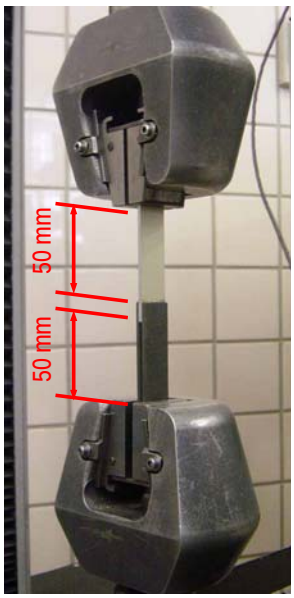

Configuration	$L_{overlap}$	Al.	τ_R (MPa)	std. dev. (MPa)	VC(%)
1) Al(3.2 mm)-$[0]_8$	12.5	A	22.26	0.65	2.94
1) Al(3.2 mm)-$[0]_8$	12.5	D	22.03	1.04	4.73
2) Al(3.2 mm)-$[0]_{12}$	12.5	A	21.85	3.73	17.07
2) Al(3.2 mm)-$[0]_{12}$	12.5	D	23.30	4.36	18.70
3) Al(3.2 mm)-$[0]_{16}$	12.5	A	26.44	1.88	7.11
3) Al(3.2 mm)-$[0]_{16}$	12.5	D	21.08	1.77	8.39
4) Al(1.6 mm)-$[0]_8$	12.5	A	22.03	2.80	12.70
4) Al(1.6 mm)-$[0]_8$	12.5	D	17.97	2.98	16.60
5) Al(1.6 mm)-$[0]_{12}$	12.5	A	21.76	1.27	5.85
5) Al(1.6 mm)-$[0]_{12}$	12.5	D	24.44	0.6	2.47
6) Al(3.2 mm)-$[0_2/90_2]_s$	12.5	A	25.01	1.20	4.81
6) Al(3.2 mm)-$[0_2/90_2]_s$	12.5	D	25.56	2.13	8.35
7) Al(3.2 mm)-$[0_3/90_3]_s$	12.5	A	26.38	1.65	6.24
7) Al(3.2 mm)-$[0_3/90_3]_s$	12.5	D	25.56	1.17	4.58
8) Al(1.6 mm)-$[0_2/90_2]_s$	12.5	A	18.43	3.82	6.73
8) Al(1.6 mm)-$[0_2/90_2]_s$	12.5	D	19.70	4.34	5.01
9) Al(1.6 mm)-$[0_3/90_3]_s$	12.5	A	20.91	0.12	0.56
9) Al(1.6 mm)-$[0_3/90_3]_s$	12.5	D	21.75	0.57	2.63
10) Al(3.2)-Al (1.6)	12.5	A	23.34	1.15	4.92
10) Al(3.2)-Al (1.6)	12.5	D	22.98	1.37	5.96
11) Al(3.2 mm)-$[0]_{12}$	20.0	A	26.20	2.06	7.86
11) Al(3.2 mm)-$[0]_{12}$	20.0	D	24.75	2.71	10.94

Table 4.- Detail of the double-lap shear test in tension, and summary of results.

For each configuration, 5 specimens were tested, the mean value of the apparent shear strength (τ_R), the standard deviation and variation coefficient (VC%) having been evaluated and presented in Table 4. Configurations 2 and 4 were observed to have high dispersion (VC%) while the rest of configurations presented good VC values for comparison purposes. Some additional tests were carried out at partial loadings (up to 90% of the observed mean value of the apparent shear strength) in order to check if a preliminary damage at the corners can be observed prior to the final catastrophic failure. Some of these inspections, for configurations 2 and 11 (both having 3.2 mm aluminium and $[0]_{12}$ unidirectional CFRP laminate, with the only difference in the overlap length, respectively 12.5 and 20 mm) are shown in Figure 4. No damage has been observed in the neighbourhood of the corner tips.

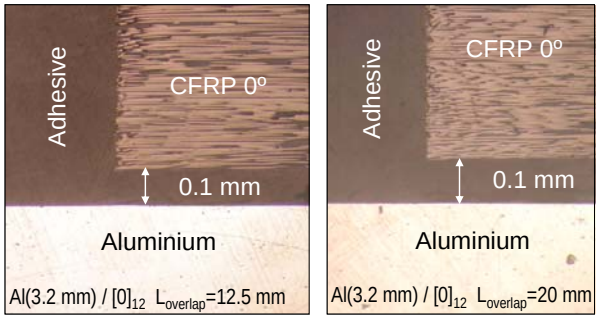

Figure 4.- Detail of corner #1 at partial loading for configurations 2 and 11.

4.- REPRESENTATIVITY OF THE SINGULAR STRESS STATE IN FAILURE

In this section the analysis of numerical and experimental results will be performed first. Then, the comparison of tendencies in both numerical and experimental results will be carried out to investigate the suitability of the parameters defining the local (singular) stress state for its possible use in the proposals of failure criteria.

4.1.- Numerical results.

From Table 3 we can observe that:

- For corner #1, all K_k values are similar in 3.2 mm Al configurations and a 40%~50% lower than K_k values for 1.6 mm Al configurations, which are also similar among them. In the following table this fact can be clearly observed for K_1 values, the reference values for 3.2 and 1.6 mm configurations being respectively configurations 1 and 4.

Configuration	1*	2	3	6	7	4*	5	8	9
Differences in K_1 (%)	0	-3.33	-2.7	-7.97	-5.91	0	-7.04	-3.23	-2

** The reference for 2, 3, 6 y 7 is conf. 1, for 5, 8 y 9 is conf. 4*

- For corner #2, the same trend is observed with same relative values for 3.2 mm and 1.6 mm configurations, having similar values in their groups and 40%~50% differences between these two groups, higher values being observed for the 1.6 mm Al configurations. In the following table, values for K_1 are presented.

Configuration	1*	2	3	6	7	4*	5	8	9
Differences in K_1 (%)	0	0.589	0.477	22.19	18.31	0	2.881	25.18	25.77

** The reference for 2, 3, 6 y 7 is conf. 1, for 5, 8 y 9 is conf. 4*

- Corner #3 appears only in these configurations having $[0_n/90_n]_s$ laminates, but the same general trend is observed. It is also clear the influence of the number of layers $[0_2/90_2]_s$ *vs.* $[0_3/90_3]_s$ in the value for K_1 is higher for the $[0_2/90_2]_s$ configurations. This effect was not observed in the $[0]_n$ laminates, the number of plies not being relevant for significant variations of K_1.

The observed tendencies can be easily justified:

- For corner #1, no significant changes appear with either the number of 0º plies or the stacking sequence, but only with the Al thickness. A satisfactory explanation is the high difference in the stiffness of both adherents. Three unidirectional laminates $[0]_8$, $[0]_{12}$ and $[0]_{16}$ were used. Shear stresses in the adhesive are higher at the overlap end with the lower stiffness. The most balanced configuration (Al 3.2 mm / CFRP $[0]_8$) is still very unbalanced, and additional increases in the number of CFRP plies just make the shear stress distribution to be more severe. However, changes in the Al thickness, the softer adherent greatly affect the stiffness ratio and the shear stress distribution.
- In corner #2 the explanation is basically the same, but the dependency observed with the stacking sequence is due to the local load transmission through the adhesive fillet, greatly affected by the presence of the 90º layer. Anyway, the tendency is not as clear as in the former case.

Configurations 2 and 11 are equal with the only difference of the lap length. No significant differences have been observed in the K_k values with the exception of corner 2, where K_1 shows a 18% variation.

4.2.- Experimental results.

With reference to results in Table 4, no significant differences were observed in the surface treatment (Anodized or Scaled) in the present static testing, although they could be expected to appear in fatigue testing. There is a clear influence of the Al thickness in the experimental results, which can be observed in the configuration pairs 6-8, and 7-9. In the following table, the results obtained for τ_R have been compared for $[0_n/90_n]_s$ (n=2,3) configurations with 1.6 and 3.2 mm Al. The values are 15%~26% lower in configurations having 1.6 mm Al.

	$[0_2/90_2]_s$-Al(A)	$[0_3/90_3]_s$-Al(A)	$[0_2/90_2]_s$-Al(D)	$[0_3/90_3]_s$-Al(D)
Al. 3.2 mm	25.01	26.38	25.56	25.56
Al. 1.6 mm	18.43 (↓26%)	20.91 (↓21%)	19.70 (↓23%)	21.75 (↓15%)

The influence of the stacking sequence on the experimental results is significant for configurations having 3.2 mm Al thickness, while this influence is not clear in configurations with 1.6 mm Al, as shown in the following table. In the former case, configurations with $[0_n/90_n]_s$ (n=2,3) show higher (10%~21%) τ_R values when compared with the corresponding $[0]_n$ (n=8,12) configurations.

		$[0]_8$	$[0_2/90_2]_s$	$[0]_{12}$	$[0_3/90_3]_s$
Al (3.2 mm)	A	22.26	25.01 (↑12%)	21.85	26.38 (↑21%)
	D	22.03	25.56 (↑16%)	23.30	25.56 (↑10%)
Al (1.6 mm)	A	22.03	18.43	21.76	20.91
	D	17.97	19.70	24.44	21.75

The influence of the overlap length on the experimental results is clear: the failure load F(KN) clearly increases (71%~93%) from $L_{overlap}$=12.5 mm to $L_{overlap}$=20.0 mm, as well as the apparent shear strength (τ_R) (6%~20%). In the following table, all these results are summarized.

F(KN)/ τ_R(MPa)	Al(3.2)-$[0]_{12}$ ($L_{overlap}$=12.5 mm)	Al(3.2)-$[0]_{12}$ ($L_{overlap}$=20.0 mm)
Aluminium A	13.8/21.85	26.6 (↑93%)/26.20 (↑20%)
Aluminium D	14.7/23.30	25.1 (↑71%)/24.75 (↑6%)

4.3.- Numerical-experimental correlation

Surface treatment: No significant influence was observed in the experimental results of anodized or scaled aluminium plates under static load. The surface treatment was not included in the numerical models as they do not modify the stiffness properties of the materials.

Aluminium thickness: If configurations 2 and 4 are excluded due to their high VC%, the influence on the mean apparent shear strength was clearly observed between the configuration couples 6-8 and 7-9, which only differ in the aluminium thickness. The experimental variation between these configurations was around 15%~26%. The numerical models also presented a clear influence 40%~50% in the computed values of K_k. Thus, a qualitative correlation exists between experimental and numerical results.

CFRP thickness: Neither the experimental nor the numerical results show a significant influence on the laminate thickness. This lack of influence was explained by the high unbalance between both adherents in the lowest case with $[0]_8$ laminate, this unbalance was even higher with $[0]_{12}$ and $[0]_{16}$ which do not change qualitatively the unbalance of the joint. It is expected that more balanced joints would be more affected by initial changes in the CFRP thickness.

Stacking sequence: With the same number of total plies, the stacking sequence affects the tensile stiffness drastically. This fact is slightly observed in the numerical results, when comparing configurations 1-6, 2-7 and 4-8, as K_1 decreases with $[0_n/90_n]_s$ laminates instead of $[0]_n$. Experimentally, a higher failure load was observed in the $[0_n/90_n]_s$ configurations. Thus the same qualitative trend is observed between the numerical and experimental results.

Overlap length: The comparison of the results of configurations 2 and 11, which only differ in the overlap length, was not significant in the numerical results but very clear in the experimental results. The configuration with 20 mm overlap has a higher failure load. Partial load test did not show any failure at the corner tip. Thus, in this case, the qualitative trend between numerical and experimental results is not the same. Using Hart-Smith [2] approach of nominal stress values, it is obtained that only the 40% of the overlap length remain elastic in the 20 mm configuration while the 99.7% is elastic in the 12.5 mm configuration. This fact shows that configuration 11 ($L_{overlap}$=20mm) with gross yielding at both sides of the overlap zone can not fully develop a failure mechanisms based on local (singular) stress states.

5.- CONCLUSIONS

The failure of adhesively bonded joints between aluminium plates and CFRP laminates has been analyzed. Using the asymptotic fields (stresses and displacements) at the multimaterial corners as the key factor for failure initiation, a complete characterization of these corners was performed using a semi-analytic tool for the evaluation of characteristic exponents and angular shape functions and using numerical models (based on the Boundary Element Method) for the computation of the Generalized Stress Intensity Factors.

A preliminary test program was carried out using double lap shear joints loaded in tension to evaluate static failure loads and apparent shear strengths. Different combinations of Al-CFRP double lap joints were tested to study the influence on the failure load of: Al thickness, CFRP thickness, stacking sequence and overlap length.

Numerical predictions and experimental results were compared to study the suitability of a failure criteria based on the parameters which define the singular stress state at these corners. The numerical-experimental comparison has shown qualitatively the same trends with every parameter variation. Only one exception was found with overlap length variation, while a clear variation was observed in the experimental results, no significant variation was obtained in the numerical models. Using an elastic-plastic model by Hart-Smith, the yielded zone in the overlap area was determined to be in a great extent (60%) of the lap distance. With the presence of this gross yielding, failure mechanisms based on local stress states can not be developed. The numerical-experimental correlation was found to exist with low yielding extent in the adhesive layer. This fact allows failure criteria based on singular stress states to be used in this type of structures.

ACKNOWLEDGEMENTS.

This work was supported by the Spanish Ministry of Education and Science, through the Projects TRA2005-06764 and TRA2006-08077, and by the Junta de Andalucía, through the Projects of Excellence TEP1207 and TEP2045.

REFERENCES

1. Matthews,F.L.,Kilty,P.F. & Godwin,E.W.“A review of the strength of joints in fibre reinforced plastics.Part 2.Adhesively bonded joints”, *Composites* ,1982;13:29-37.
2. Hart-Smith, L. J., “Analysis and design of advanced composite bonded joints”, NASA CR-2218, 1974.
3. Leman, G. M. and Hawley, A. V. “Investigations of joints in advanced fibrous composites for aircraft structures”, *Technical Report No AFFDL-TR169-43* Vol 1 (US Air Force, June 1979).
4. Crocombe, A. D. “Global yielding as a failure criterion for bonded joints”, *International Journal of Adhesion and Adhesives*, 1989;9:145-15 .
5. Kairouz, K. C. “The influence of stacking sequence on the strength of bonded CFRP joints”, *PhD Thesis* (Imperial College, London), 1991.
6. Adams, R. D., Comyn, J. and Wake, W. C., *Structural adhesive joints in engineering* (second edition), Chapman & Hall, 1997.
7. Adams, R. D. and Mallick, V. “A method for stress analysis of lap joints”, *Journal of Adhesion*, 1992;38:199-217.

8. Fernlund, G. and Spelt, J. K. “Failure load prediction of structural adhesive joints”, *International Journal of Adhesion and Adhesives*, 1991;11: 213-220.
9. Hutchinson, J.W. and Suo, Z., Advances in Applied Mechanics 1992;29:63-191.
10. Gradin, P. “A fracture criterion for edge bonded bimaterial bodies”, *Journal of Composite Materials*, 1982;16: 448-456.
11. Groth, H. L. “Stress singularities and fracture at interface corners in bonded joints”, *Int. Journal of Adhesion and Adhesives*, 1988;8: 107-113.
12. Hattori, T. “A stress-singularity-parameter approach for evaluating the adhesive strength of single lap joints”, *JSME Int. Journal*, Series I, 1991;34:326-331.
13. Reedy, Jr., E. D. “Connection between interface corner and interfacial fracture analyses of an adhesively bonded butt joint”, *International Journal of Solids and Structures*, 2000;37:2443-2471.
14. Reedy, Jr., E. D. and Guess, T. R. “Interface corner failure analysis of joint strength: effect of adherent stiffness”, *I. Journal of Fracture*,1998;94: 305-314.
15. Lefebvre, D. R., Dillard, D. A. and Dillard, J. G. “A stress singularity approach for the predictions of fatigue crack initiation in adhesive bonds. Part 2: Experimental”, *Journal of Adhesion*, 1999;70: 139-154.
16. Quaresimin, M. and Ricotta, M. “Fatigue behaviour and damage evolution of single lap bonded joints in composite materials”, *Comp. Sci. Technology*,2006;66:176-187.
17. Leguillon, D. and Yosibash, Z. “Crack onset at a v-notch. Influence of the notch tip radius”, *International Journal of Fracture*; 2003;122:1-21.
18. Grenestedt, J. L. and Hallstrom, S. “Crack initiation from homogeneous and bimaterial corners”, *J. of Applied Mechanics*,1997;64: 811-818.
19. Laschet,G. and Stas,A. “Finite element failure prediction of adhesive joints using a simple damage model”,*Report SA-158*,Str.Aer.(University de Liege,Belgique),1992.
20. Sheppard, A., Kelly, D. and Tong, L. "A damage zone model for the failure analysis of adhesively bonded joints", *Int. J. Adhesion and Adhesives*,1998;18: 385-400.
21. Mohammed, I. and Liechti, K. M. “Cohesive zone modelling of crack nucleation at bimaterial corners”, *J. of the Mechanics and Physics of Solids*,2000;48:735-764.
22. Costabel, M. Dauge, M. and Lafranche, Y., “Fast semi-analytic computation of elastic edge singularities”, Université de Rennes I, 1998.
23. Barroso, A., Mantič, V. and París, F. “Singularity analysis of anisotropic multimaterial corners”, *Int. Journal of Fracture*,2003;119: 1-23.
24. Sinclair, G.B. “Logarithmic stress singularities resulting from various boundary conditions in angular corners of plates in extension”, *J.Appl.Mech*,1999;66:556-559.
25. Barroso, A. “Characterization of singular stress states at multimaterial corners. Application to adhesively bonded joints with composite materials”, Ph.D. Thesis (*in Spanish*), University of Seville, Spain, 2007.
26. Barroso, A., Mantič, V. and París, F. “Evaluation of generalized stress intensity factors in anisotropic elastic multimaterial corners”, *ECCM-11*, Rodhes (Greece), 2004, (on CD, paper A032).
27. Pageau, S. P., Gadi, K. S., Biggers, Jr., S. B. and Joseph, P. F. “Standardized complex and logarithmic eigensolutions for n-material wedges and junctions”, *International Journal of Fracture*,1996;77: 51-76.
28. ASTM D3528-96 (2002) *Standard Test Method for Strength Properties of Double Lap Shear Adhesive Joints by Tension Loading*.